

Complete oxidation of 1,2-dichlorobenzene over V_2O_5 -TiO₂ and MnO_x-TiO₂ aerogels

Jinsoo Choi* and Dong Jin Suh**†

*Coal Chemistry Research Project, Research Institute of Industrial Science and Technology,
Pohang, Gyeongbuk 790-330, Korea

**Clean Energy Research Center, Korea Institute of Science and Technology,
P. O. Box 131, Cheongryang, Seoul 136-791, Korea

(Received 5 January 2014 • accepted 29 April 2014)

Abstract—Catalytic destruction of 1,2-dichlorobenzene was carried out over two types of aerogels, vanadia-titania and manganese oxide-titania. Reactions were performed in a plug flow reactor in the range of 150–600 °C. Both catalysts resulted in very high selectivity to carbon oxides and produced negligible amount of hydrocarbon byproducts. Over the vanadia-titania catalysts, the chlorinated compound was relatively more efficiently destructed at lower temperature, while selectivity towards carbon dioxide was much higher over manganese oxide-titania aerogel catalysts. Vanadia-titania catalysts, regardless of the preparation methods, showed a tendency to produce carbon monoxide with 35–45% selectivity throughout the reaction temperature range while manganese oxide-titania exhibited more than 90% CO₂ selectivity at above 400 °C.

Keywords: Vanadia, Manganese Oxide, Aerogel, 1,2-Dichlorobenzene, Oxidation

INTRODUCTION

Sol-gel synthesis enables active sites to be highly dispersed on supports and induces strong interactions between these sites and the support materials [1]. Subsequent supercritical drying maintains the original structures without drastic changes to the physical properties, even after a high-temperature calcination process, which is necessary for the removal of organic residues. Aerogels are characterized by high specific surface area, mesoporosity, and the retardation of crystallization [2]. These unique properties make them ideal as catalysts and catalyst supports for application to numerous chemical reactions.

Chlorinated aromatic compounds such as furans and dioxins have been designated as human carcinogenic substances in environmental regulations. Demand for detoxification of chlorinated compounds has gradually increased, necessitating the disposal of widely used chlorinated chemical products. Various studies have been performed on photodegradation [3], biodegradation [4], thermal decomposition [5], and catalytic hydrogenation [6] or oxidation [7]. Considering reaction rate, energy consumption, and catalytic deactivation, oxidation processes using metal oxide catalysts are considered to be the optimum approach for effective removal of chlorinated compounds. Catalytic oxidation is a fast decomposition method compared to UV irradiation and biodegradation, and generates fewer chemical byproducts than pyrolysis and hydrodechlorination processes. As chlorine acts as a poisonous compound to noble metal catalysts, metal oxides could be a smart choice to extend the catalyst lifetime. This study evaluates V_2O_5 -TiO₂ and MnO_x-TiO₂ aerogels as catalysts for the complete oxidation of 1,2-dichlorobenzene.

EXPERIMENTAL

1. Catalyst Preparation

Catalysts were prepared by both conventional impregnation and sol-gel synthesis. For the impregnated V_2O_5 -TiO₂ catalysts (ImpV), an aqueous solution of ammonium metavanadate was mixed with P-25 (Degussa, 51 m² g⁻¹) titania. The resulting mixture was dried at 80 °C in an oven and calcined at 500 °C under air. Aerogels were synthesized by the addition of vanadium oxytriisopropoxide or manganese nitrate hydrate to titanium tetrabutoxide in the case of vanadia-titania (AeroV) and manganese oxide-titania (AeroMn) aerogels, respectively. Ethanol solutions of precursors were mixed with nitric acid and water, and agitated until gelation occurred. Monolithic gels were dried by the low temperature supercritical processes using carbon dioxide. Dried aerogels were thermally treated at 300 °C under helium and 500 °C in an air environment. To enhance the amount of vanadia at the outer-most surface of titania, prehydrolysis of titanium tetrabutoxide was carried out before adding vanadium oxytriisopropoxide (Pre-AeroV). Detailed procedures can be found elsewhere [8,9].

2. Characterization of Catalysts

BET surface area, total pore volume and pore size distributions were measured by nitrogen adsorption-desorption at –196 °C with Micromeritics ASAP 2000 and 2010 instruments. The mesopore size distributions were calculated from the desorption isotherms. All the samples were pre-treated in vacuum at 120 °C overnight prior to the measurement.

A transmission electron microscope (Philips CM30) was used to distinguish particle sizes. X-ray powder diffraction patterns for identifying crystalline phases were obtained with a Rigaku D/MAX-III A diffractometer using CuK α irradiation. The Raman (Jobin-Yvon T64000) spectra were taken using 50 mW of the 514.5 nm line of an Ar ion laser. The signal was dispersed by a Spex 0.6 m

†To whom correspondence should be addressed.

E-mail: djsuh@kist.re.kr

Copyright by The Korean Institute of Chemical Engineers.

triple spectrometer and detected with a charge coupled device detector. Temperature programmed reduction was carried out with 0.1 g of the catalysts heated at $5\text{ }^\circ\text{C min}^{-1}$ under 5% hydrogen in argon at 30 ml min^{-1} . A thermal conductivity detector was used to monitor the hydrogen consumption. Using an SSI 2803-S spectrometer, X-ray photoelectron spectrograms were acquired to confirm the oxidation state of the additives.

3. Reaction Experiment

The catalytic activities were measured in a quartz fixed-bed flow reactor (1 cm inner diameter) with 75 mg or 0.5 g of catalysts. 1,2-Dichlorobenzene was placed in a saturator and introduced to the reactor via the passage of nitrogen. Its concentration was maintained by controlling the temperature of the saturator. Gas lines were placed in a heating chamber to avoid condensation of the reactant. To simulate the composition of air, the flow rates of nitrogen and oxygen were adjusted to 40 and 10 ml min^{-1} , respectively. Nitrogen was used as a carrier gas for 1,2-dichlorobenzene and introduced to the heating chamber directly. Oxygen was mixed with nitrogen in the heating chamber before the catalytic bed. Reaction temperature was controlled at $150\text{--}600\text{ }^\circ\text{C}$ with a $50\text{ }^\circ\text{C}$ increment and held for two hours at each temperature. The catalytic activity measurements were made at an overall space velocity of $3,000\text{--}50,000\text{ hr}^{-1}$ and at a concentration of 1,000 ppm of 1,2-dichlorobenzene.

The reactor effluent gas was analyzed by using two gas chromatographs (HP6890, Younglin M600D) equipped with flame ionization detectors: one with a capillary column ($30\text{ m}\times 0.32\text{ mm DB-5}$, $0.25\text{ }\mu\text{m}$) for 1,2-dichlorobenzene and the other with a packed column ($6'\times 1/8''\times 0.085''\text{ SS}$, Carbosphere 80/100) with a methanator containing commercial nickel catalyst for CO and CO_2 .

RESULTS AND DISCUSSION

1. Characteristics of the Catalysts

Textural properties were measured by N_2 adsorption, as given in Table 1. Both $\text{V}_2\text{O}_5\text{-TiO}_2$ and $\text{MnO}_x\text{-TiO}_2$ aerogels showed two- to three-times higher specific surface area and total pore volume than

Table 1. BET surface area (S_{BET}), total pore volume (V_p), and average pore size (D_p) of $\text{V}_2\text{O}_5\text{-TiO}_2$ and $\text{MnO}_x\text{-TiO}_2$ catalysts calcined at $500\text{ }^\circ\text{C}$

Sample name	Content	S_{BET} (m^2/g)	V_p (cc/g)	D_p (nm)
AeroTi	TiO_2	189	0.67	14.1
ImpV5	5 wt% V_2O_5	55	0.32	23.2
ImpV10	10 wt% V_2O_5	42	0.26	24.8
AeroV5	5 wt% V_2O_5	153	0.57	14.9
AeroV10	10 wt% V_2O_5	127	0.83	25.3
AeroV15	15 wt% V_2O_5	29	0.18	25.2
AeroMn5	5 wt% Mn	153	0.84	21.1
AeroMn10	10 wt% Mn	166	0.79	19.0
AeroMn15	15 wt% Mn	37	0.19	20.0
Pre-AeroV5	5 wt% V_2O_5	153	0.65	17.0
Pre-AeroV10	10 wt% V_2O_5	110	0.56	20.2
Pre-AeroV15	15 wt% V_2O_5	23	0.13	22.7

the impregnated catalysts, which exhibited quite similar values to those of the support material, P-25 TiO_2 . The physical properties are thus significantly dependent on the preparation methods.

Since the specific surface area of a support determines the amount of active sites to be loaded with catalytic materials, aerogels with high surface area can be particularly advantageous supports for increased loading of active sites without bulk-sized crystal formation. For vanadia, based on the theoretical calculation for a surface area of $10\text{ m}^2\text{ g}^{-1}$, the weight percentages of monolayers of monovanadate and polyvanadate are 0.35 and 1.05 wt%, respectively [10]. In this calculation, impregnated catalysts tend to have bulk-phase vanadia crystalline when the weight percentage of the monolayer reaches 6 wt% while aerogels can be basically loaded two- to three-times more without the crystal phase. At higher loadings of vanadia, however, there were drastic decreases in the specific surface area and total pore volume when vanadia loading was increased from 10 (AeroV10) to 15 wt% (AeroV15). This is because entrapped

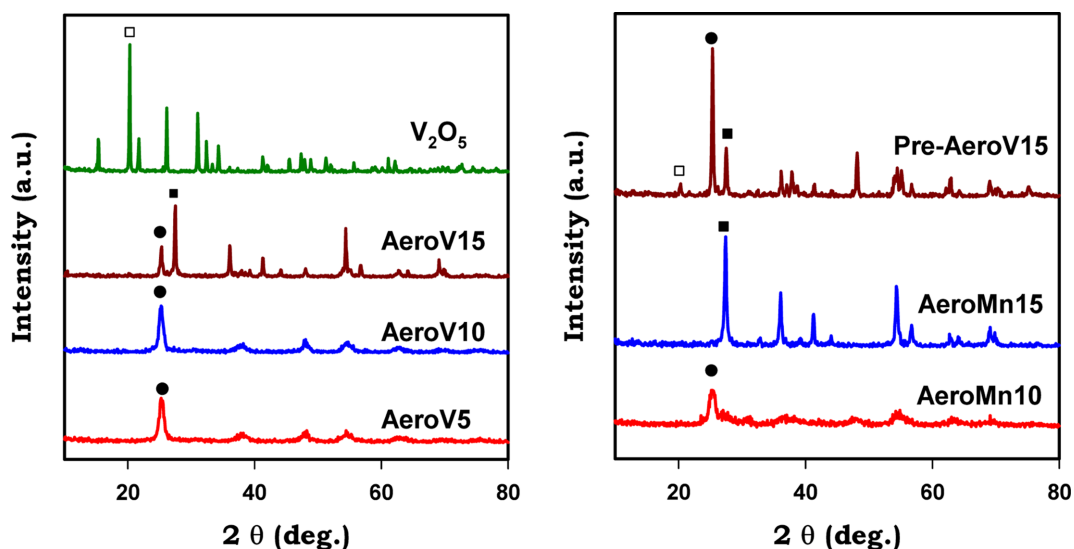


Fig. 1. XRD patterns of synthesized aerogels with indication of the highest peaks for V_2O_5 (\square), TiO_2 rutile (\blacksquare), and TiO_2 anatase (\bullet) crystalline. All the samples were calcined at $500\text{ }^\circ\text{C}$.

vanadia acted as an adhesive in between the titania crystallites, resulting in increased particle size and/or phase transformation of titania for thermodynamic stabilization [11]. Consequently, bulk vanadia appeared in accordance with how well vanadia was dispersed. MnO_x-TiO₂ aerogels showed a similar trend (AeroMn10 and 15).

Primary particle sizes also varied considerably depending on the preparation methods. Aerogels showed uniformly developed particles of 10 nm, while impregnated samples displayed irregular sizes. Potential benefits can arise from the capacity of scattered nano-sized particles to induce not only strong interaction between metal oxides but also retardation of crystallization, owing to the consequent low surface density of vanadia or manganese oxide [12].

Crystallinity of titania largely depended on vanadia or manganese oxide content in the aerogels. Fig. 1 shows X-ray diffraction patterns of V_2O_5 -TiO₂ and MnO_x-TiO₂ aerogels calcined at 500 °C. The prevailing crystallite of TiO₂ was anatase phase until the loading reached 10 wt% with negligible V_2O_5 and MnO_x crystallite. When the loading reached 15 wt%, abrupt phase transitions occurred, as observed in AeroV15 and AeroMn15 catalysts. Unique characteristics of the sol-gel method, which uses a homogeneously mixed metallic solution, unavoidably resulted in the insertion of additive species into the titania structure and the encapsulated additives drove TiO₂ from an anatase phase to a thermodynamically more stable rutile phase.

Since anatase phase plays an important role of forming a stable vanadia monolayer [13] and enhancing oxygen uptake [14], the crystallite of TiO₂ is a crucial factor for catalytic activity in complete oxidation. For this reason, the XRD results suggest that the optimum loading of vanadia is approximately 10 wt%.

To diminish the encapsulation effect through the sol-gel preparation, prehydrolysis of the Ti solution was conducted prior to the cogelation process. The obtained aerogel catalyst (Pre-AeroV15) was found to maintain an anatase phase with enriched vanadia at the outer surface of titania, which induced crystallization of vanadia in a bulk phase at high loadings of V species.

Fig. 2 represents various chemical states of surface vanadia observed through Raman spectroscopy. Structures are often distinguished as monovanadate, bulk vanadia, and polyvanadates, which

are assigned at Raman shifts of 1,030, 995, and 920 cm^{-1} , respectively [15]. Among these, strongly interacting vanadia known as monovanadate and polyvanadate usually exhibits excellent oxidation reactivity [11].

As vanadia loading is a critical factor for evaluating the surface coverage, as determined in theoretical calculations, a bulk vanadia peak at 995 cm^{-1} started to appear in ImpV5 and grew intensely in ImpV8. This peak, however, did not appear at all in aerogel catalysts even when the vanadia content was increased to 15 wt% (AeroV15). The sol-gel process employs a homogeneous mixed solution to produce polymeric gel networks; thus the vanadia is located not only on the surface of titania but also in the titania structure. The inherent surface dominancy of vanadia on impregnated catalysts was totally different from vanadia occlusion in aerogels. The amount of vanadia existing on the surface can be roughly determined by the TPR method, as will be shown later.

Low loading of vanadia (AeroV5) leads mostly to a monovanadate at a Raman shift of 1,030 cm^{-1} due to highly dispersed characteristics, and higher loading (AeroV10) tends to transform monovanadate into polyvanadates, observed at a shift of 920 cm^{-1} . From these results, we may conclude that the formation of different surface vanadates cannot be precisely controlled according to vanadia loading. A trend of structure dominancy, however, was observed as a function of vanadia loading in aerogels.

Hydrogen consumption profiles were acquired from temperature programmed reduction (TPR) by hydrogen, as presented in Fig. 3. When reducible metal oxides such as vanadia and manganese oxides are supported on, their reduction temperatures are often shifted to lower temperatures. Considering the TPR peaks for pure V_2O_5 (peaks at ca. 650, 700, and 800 °C) [16] and for MnO_x (Mn₃O₄, Mn₂O₃ - single peak at ca. 520 °C) [17], it is evident that these two metal oxides when presented as composite materials with titania have strong interactions with TiO₂, likely to lose their oxygen at various temperatures.

Since no peaks for bulk vanadia were observed for AeroV15 in the XRD and the Raman spectrum, as shown in Fig. 1 and Fig. 2(b), different maximum temperatures in TPR should result from the effect of interactions between vanadia and titania. Vanadium content

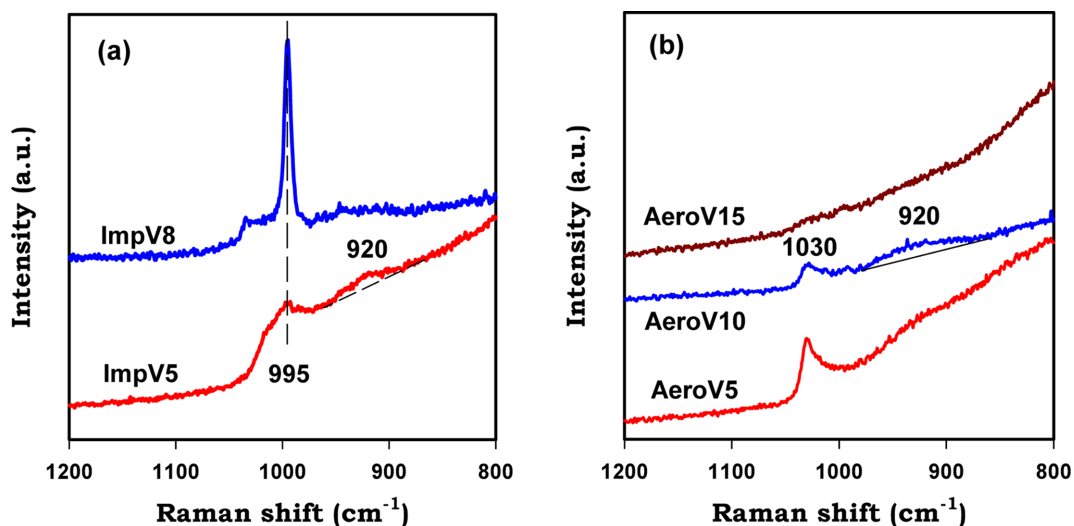


Fig. 2. Raman spectra of (a) ImpV and (b) AeroV catalysts.

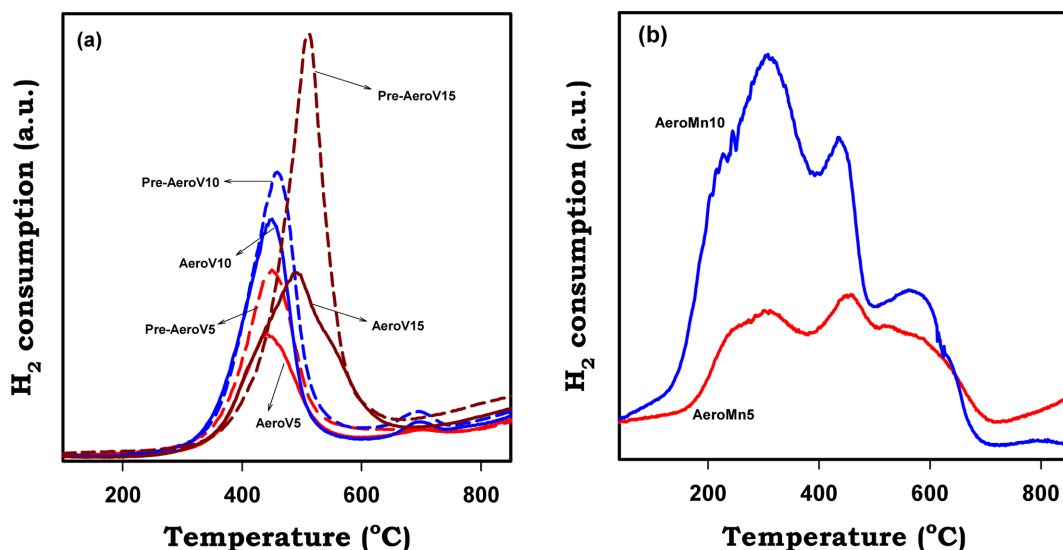


Fig. 3. TPR spectra of (a) AeroV, Pre-AeroV, and (b) AeroMn catalysts.

does not appear to be critical for the formation of bulk vanadia, especially on aerogel catalysts, due to its inherent homogeneity of the aerogel. Meanwhile, the rutile phase of titania was highly developed, as illustrated in Fig. 1. In light of the observation that aerogel catalysts with low surface area of less than $30 \text{ m}^2 \text{ g}^{-1}$ exhibited higher reduction temperature, there should be much less interaction between vanadia and titania due to the crystalline phase.

As a result, strongly interacting vanadia were well developed up to 10 wt%. Furthermore, the peak at 450°C appeared to be attributable to strongly interacting surface vanadates with anatase phase. The oxidation state of vanadium was maintained at V^{5+} regardless of the interaction strength when the binding energies of V^{3+} , V^{4+} , and V^{5+} were assigned at 515, 516, and 518 eV, respectively, as can be observed from the XPS results presented in Fig. 4(a) [18].

Two methods were used for the preparation of vanadia aerogels, conventional sol-gel synthesis (one step method, AeroV) and prehydrolysis (two step method, Pre-AeroV). Hydrogen consumption

was measured for two aerogel catalysts, AeroV and Pre-AeroV (Fig. 3(a)), to clarify not only the strength of the interactions, but also the effect of vanadia enrichment at the outermost surface of the catalysts. Peak intensity was highly intensified by the prehydrolysis preparation method while the position remained the same. This indicates that the amount of vanadia exposed on the surface of the catalyst increased, since its reducibility is proportional only to the vanadia.

Vanadium insertion in composite aerogels can also be verified by hydrogen consumption, because the reduction of inserted vanadia is hampered by the encircled support materials. As the vanadia content was increased, the ratio of the hydrogen consumption obtained from the major peaks for AeroV5/AeroV10/AeroV15 became 1/1.63/1.99. The relative amount of hydrogen consumed for a unit wt% of vanadia decreased with an increase of vanadia content. This approach allows for a direct comparison of various sol-gel methods designed for surface enrichment of vanadia species. The limitation of the entrapping phenomenon was overcome by using the

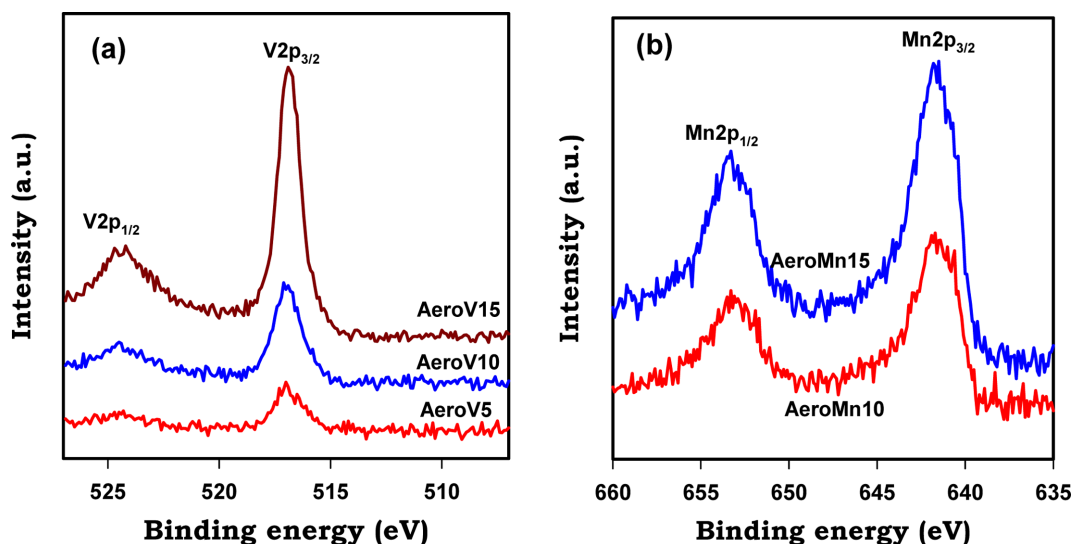


Fig. 4. XPS spectra of (a) AeroV and (b) AeroMn.

prehydrolysis method. However, this method also resulted in a large extent of vanadia entrapping resulting in peak ratios for Pre-AeroV5/Pre-AeroV10/Pre-AeroV15 of 1/1.52/2.02.

AeroMn samples showed more than three reduction peaks, at ca. 310, 450, and 560 °C, with a shoulder at 250 °C. These results are not in good agreement with those of a previous study for highly dispersed Mn (390 °C) or bulk MnO_x (470 °C) [19], but they nevertheless verify that Mn also highly interacts with titania. When manganese oxide was increased from 5 to 10 wt%, the relative peak intensity at 310 °C became much higher than that at 450 and 560 °C. This implies that the reductions were not performed in a series with changing oxidation states but in an individual reduction process for each species. Since MnO_x - TiO_2 aerogels were thermally treated at 500 °C, Mn_2O_3 -like oxide was likely to be predominant. From the viewpoint of general transfer in the oxidation state, MnO_2 is easily transformed into Mn_2O_3 , which is the most thermodynamically stable form, after thermal treatment at 500 °C in an air environment. Mn_3O_4 and MnO can be found at much higher temperatures of 900 and 1,700 °C, respectively [20]. XPS results, however, as given in Fig. 4(b), did not firmly indicate if a certain state was dominant, considering that Mn^{4+} as found in MnO_2 appeared at 642-642.7 eV, Mn^{3+} in Mn_3O_4 at 641.2 eV, Mn_2O_3 at 641.9 eV, and Mn^{2+} in MnO

at 640.6-641.7 eV [21].

2. Activity Measurements

The catalytic activities were evaluated in a reaction temperature range of 150-600 °C under an air environment. Gas chromatography was used for the calculation of conversions and yields of each component with carbon balances. The amount of byproducts other than carbon oxides was negligible. The byproducts were not chlorinated aromatic compounds such as chlorobenzene, 1,3-dichlorobenzene or 1,4-dichlorobenzene, and the activities were maintained even after 48 hrs. According to Krishnamoorthy and Amiridis, the byproducts are likely carboxylate, carbonate, maleate, and phenolate species [22].

In binary systems, the usual active sites are highly dispersed and/or strongly interacting metal oxides. It has been widely suggested that, on vanadia-titania, surface vanadates known as mono- and polyvanadates have excellent oxidation activity in both partial and complete oxidation [23,24]. Notably, highly dispersed manganese oxide showed great redox properties in a MnO_x/TiO_2 system [25]. In addition to the active components, the interacting supports also might play an important role in enhancing the catalytic activity. The activities were in the order of $TiO_2 > Al_2O_3 > SiO_2$, showing good agreement with the results of previous studies [25,26]. Furthermore, TiO_2

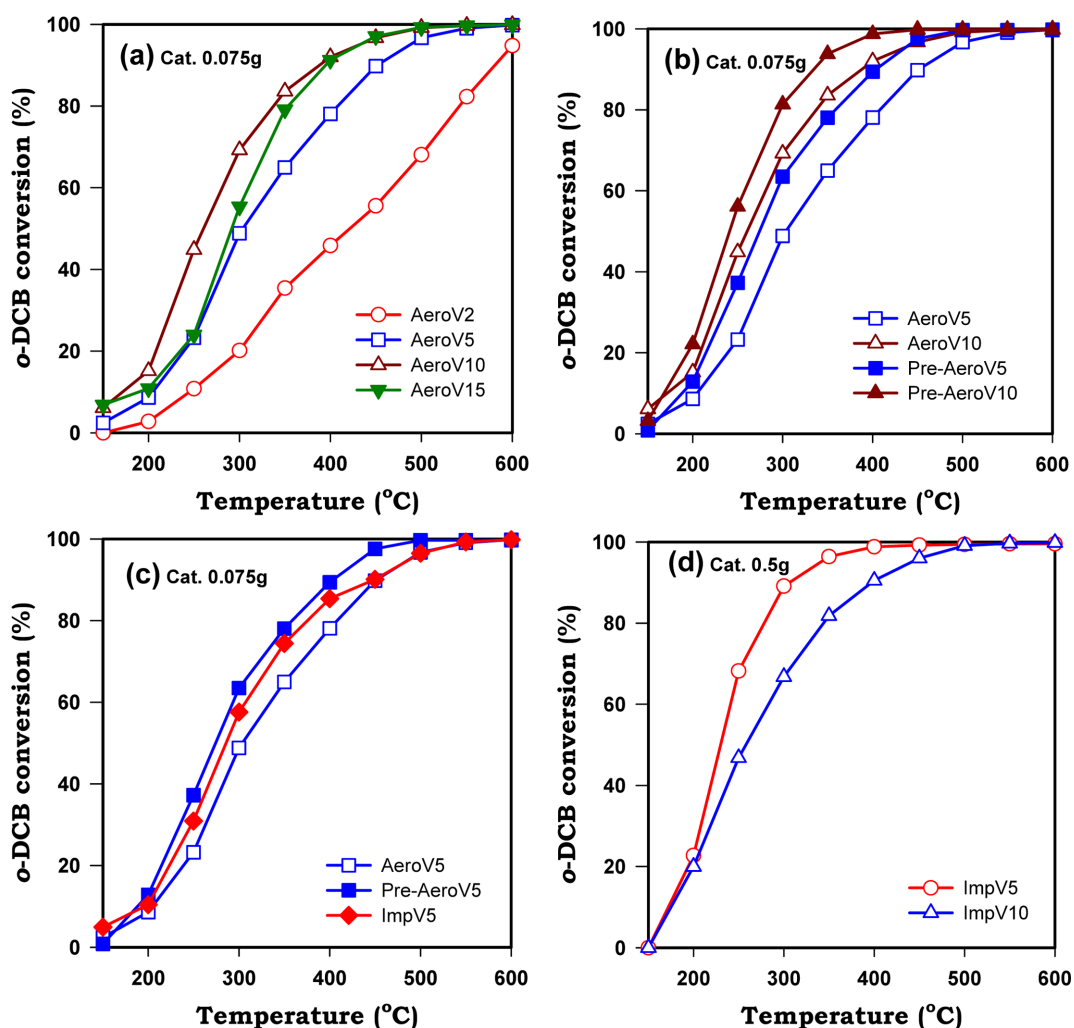


Fig. 5. Conversion of 1,2-dichlorobenzene over vanadium based catalysts as a function of temperature.

anatase phase was also a crucial factor for higher oxidation activity, because the interactions of vanadia were generally more enhanced on anatase than on rutile phase. This result was confirmed by a decrease of activity over ImpV10 compared to that over AeroV15, where the latter showed negligible bulk vanadia, higher vanadia content, and a large portion of rutile phase.

Both sol-gel derived vanadia and manganese oxide aerogels showed certain limitations in terms of the capacity of utilizing loading amounts to maintain unique properties of aerogels. Catalytic activities gradually increased as the loading of the active components was raised up to 10 wt%. However, when the loading reached 15 wt%, the catalytic activity was reduced, as shown in Fig. 5(a). Limitations were more clearly observed on impregnated catalysts, as shown in Fig. 5(d); that is, ImpV10 showed lower activity than ImpV5. This is because bulk vanadia started to appear in ImpV5 and developed much more in ImpV10. These results clearly indicate that greater dispersion of active components on titania provides better performance.

Prehydrolysis enabled the surface content of vanadia to be increased, and the catalytic activity consequently improved, as illustrated in Fig. 5(b). While conventional sol-gel methods inevitably resulted in the encapsulation of active components due to the homogeneous liquid phase preparation, prehydrolysis mitigated this phenomenon to some extent. Due to the same effect of encapsulation, the conventionally prepared vanadia-titania aerogel, AeroV5, showed slightly lower activity than ImpV5, as illustrated in Fig. 5(c).

In summary, catalytic activities with the same loading of vanadia were in the order of Pre-AeroV5>ImpV5>AeroV5 due to the partial encapsulation. On the other hand, high dispersion rendered the aerogel catalysts more active, and the catalytic activities were in the order of Pre-AeroV10>AeroV10>>ImpV5>ImpV10.

Catalytic behaviors of AeroV and AeroMn were somewhat different in terms of selectivity. AeroMn was found to have higher CO₂ selectivity, as shown in Fig. 6, while AeroV exhibited higher conversion of 1,2-dichlorobenzene at low temperatures. However, it is worthwhile to note that, for xylene oxidation, the selectivity to carbon dioxide exceeded over 95% on vanadia catalysts [27]. Consid-

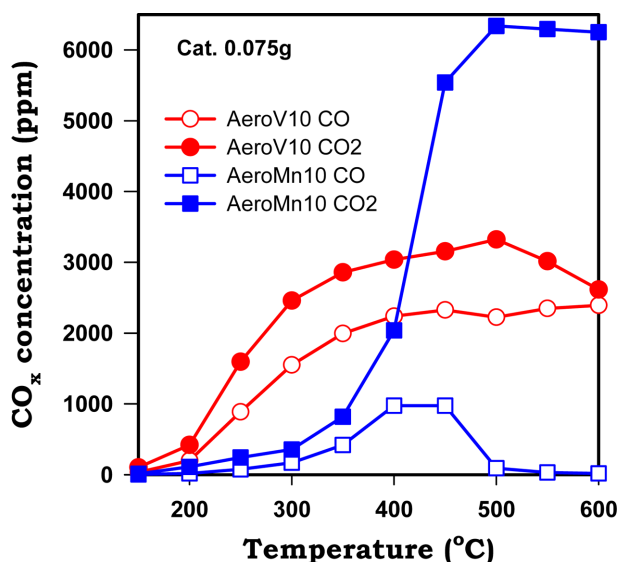


Fig. 6. Selectivity to carbon oxides for AeroV10 and AeroMn10.

ering the difference between dichlorobenzene and xylene, the chlorine atom could play a crucial role.

The following is a plausible explanation for this shift to carbon dioxide. These dominant reactions for complete oxidation likely involve a different bonding enthalpy between the metal and the chlorine compound. In other words, a high activation energy barrier is the main cause of the shift. Surface chlorine blocks oxygen adsorption and consequently prevents carbon monoxide from having an opportunity to react with adsorbed oxygen. As the reaction temperature is raised, the activation energy barrier on manganese oxide is more easily overcome due to its lower bonding enthalpy to chlorine. Bonding enthalpies of V-Cl and Mn-Cl are 477 ± 63 kJ mol⁻¹ and 360.7 ± 9.6 kJ mol⁻¹, respectively. As metal-chlorine bonds were formed during oxidative destruction of chlorobenzene [19], their strengths could be an essential factor. Consequently, at high reaction temperatures above 450 °C, Mn-Cl bonds could be dissociated by thermal energy, which gives oxygen the chance to be chemisorbed.

CONCLUSIONS

Sol-gel derived vanadia-titania and manganese oxide-titania aerogel catalysts have advantages of flexibility in preparation as well as catalytically favorable physical properties, such as high specific surface area and a highly dispersed active component. Anatase phase was maintained up to a loading of 10 wt% due to the effect of retarded crystallization. Prehydrolysis enhanced the amount of active sites at the outermost surface of titania with less developed rutile phase.

Vanadia and manganese oxide exhibited different selectivity patterns in catalytic performance. Although the results did not provide direct information, oxidative destruction of xylene and dichlorobenzene over vanadia-titania composite aerogels demonstrated that chlorine was a major factor accounting for the difference in selectivities. Both AeroV and AeroMn catalysts showed high activity without deactivation for 48 hours on stream and produced only trace amounts of byproducts. Loadings should be limited to no greater than 10 wt%, because TiO₂ phase transforms into a rutile structure and there is an increase in the amount of byproducts beyond this level.

ACKNOWLEDGEMENTS

This work was supported by the Korea Institute of Science and Technology (KIST).

REFERENCES

1. S. Krompiec, J. Mrowiec-Bialon, K. Skutil, A. Dukowicz, L. Pajak and A. B. Jarzebski, *J. Non-Cryst. Solids*, **315**, 297 (2003).
2. J. Wang, S. Uma and K. J. Klabunde, *Micropor. Mesopor. Mater.*, **75**, 143 (2004).
3. C. Guillard, J. Disdier, C. Monnet, J. Dussaud, S. Malato, J. Blanco, M. I. Maldonado and J.-M. Herrmann, *Appl. Catal. B: Environ.*, **46**, 319 (2003).
4. J. Borja, D. M. Taleon, J. Auresenia and S. Gallardo, *Proc. Biochem.*, **40**, 1999 (2005).
5. G. Rouzet, D. Schwartz, R. Gadiou and L. Delfosse, *J. Anal. Appl. Pyrol.*, **57**, 153 (2001).

6. Y. Hashimoto and A. Ayame, *Appl. Catal. A: Gen.*, **250**, 247 (2003).
7. X. Ma, X. Feng, J. Guo, H. Cao, X. Suo, H. Sun and M. Zheng, *Appl. Catal. B: Environ.*, **147**, 666 (2014).
8. D. J. Suh, T.-J. Park, Y.-H. Yoon and J. Choi, Korea Patent 10-2005-0002502, WO/2006/075840.
9. D. J. Suh, T.-J. Park, Y.-H. Yoon and J. Choi, Korea Patent 10-2004-0100192, WO/2006/059838.
10. G. Centi, *Appl. Catal. A: Gen.*, **147**, 267 (1996).
11. J. Choi, C. B. Shin, T.-J. Park and D. J. Suh, *Appl. Catal. A: Gen.*, **311**, 105 (2006).
12. J. Choi and D. J. Suh, *Catal. Surv. Asia*, **11**, 123 (2007).
13. G. C. Bond, *Appl. Catal. A: Gen.*, **157**, 91 (1997).
14. K. V. R. Chary, G. Kishan, K. S. Lakshmi and K. Ramesh, *Langmuir*, **16**, 7192 (2000).
15. D. A. Bulushev, L. Kiwi-Minsker, F. Rainone and A. Renken, *J. Catal.*, **205**, 115 (2002).
16. S. Shylesh, S. P. Mirajkar and A. P. Singh, *J. Mol. Catal. A*, **239**, 57 (2005).
17. Y.-F. Han, F. Chen, Z. Zhong, K. Ramesh, L. Chen and E. Widjaja, *J. Phys. Chem. B*, **110**, 24450 (2006).
18. M. Faraldos, J. A. Anderson, M. A. Banières, J. L. G. Fierro and S. W. Weller, *J. Catal.*, **168**, 110 (1997).
19. Y. Liu, Z. Wei, Z. Feng, M. Luo, P. Ying and C. Li, *J. Catal.*, **202**, 200 (2001).
20. E. R. Stobbe, B. A. de Boer and J. W. Geus, *Catal. Today*, **47**, 161 (1999).
21. A. Chen, H. Xu, Y. Yue, W. Hua, W. Shen and Z. Gao, *J. Mol. Catal. A*, **203**, 299 (2003).
22. S. Krishnamoorthy and M. D. Amiridis, *Catal. Today*, **51**, 203 (1999).
23. C. Freitag, S. Besselmann, E. Löffler, W. Grunert, F. Rosowski and M. Muhler, *Catal. Today*, **91-92**, 143 (2004).
24. B. M. Weckhuysen and D. E. Keller, *Catal. Today*, **78**, 25 (2003).
25. Y. Liu, M. Luo, Z. Wei, Q. Xin, P. Ying and C. Li, *Appl. Catal. B: Environ.*, **29**, 61 (2001).
26. F. Arena, F. Frusteri and A. Parmaliana, *Appl. Catal. A: Gen.*, **176**, 189 (1999).
27. J. Choi and D. J. Suh, *Unpublished results* (2005).